Research Article

Guo Li*, Zheng Zhuang, Yajun Lv, Kejin Wang, and David Hui

Enhancing carbonation and chloride resistance of autoclaved concrete by incorporating nano-$CaCO_3$

https://doi.org/10.1515/ntrev-2020-0078
received September 14, 2020; accepted September 29, 2020

Abstract: Three nano-$CaCO_3$ (NC) replacement levels of 1, 2, and 3% (by weight of cement) were utilized in autoclaved concrete. The accelerated carbonation depth and Coulomb electric fluxes of the hardened concrete were tested periodically at the ages of 28, 90, 180, and 300 days. In addition, X-ray diffraction, thermogravimetry, and mercury intrusion porosimetry were also performed to study changes in the hydration products of cement and microscopic pore structure of concrete under autoclave curing. Results indicated that a suitable level of NC replacement exerts filling and accelerating effects, promotes the generation of cement hydration products, reduces porosity, and refines the micropores of autoclaved concrete. These effects substantially enhanced the carbonation and chloride resistance of the autoclaved concrete and endowed the material with resistances approaching or exceeding that of standard cured concrete. Among the three NC replacement ratios, the 3% NC replacement was the optimal dosage for improving the long-term carbonation and chloride resistance of concrete.

Keywords: nano-$CaCO_3$, autoclaved concrete, carbonation, chloride resistance, optimal dosage

*** Corresponding author: Guo Li,** Jiangsu Key Laboratory of Environmental Impact and Structural Safety in Engineering, China University of Mining and Technology, Xuzhou, 221116, China, e-mail: guoli@cumt.edu.cn
Zheng Zhuang: School of Mechanics and Civil Engineering, China University of Mining and Technology, Xuzhou, 221116, China
Yajun Lv: School of Civil Engineering, Shenzhen University, Shenzhen, 518061, China
Kejin Wang: Department of Civil, Construction & Environmental Engineering, Iowa State University, Ames, IA 50011, United States of America
David Hui: Department of Mechanical Engineering, The University of New Orleans, New Orleans, LA, 70148, United States of America

1 Introduction

Autoclave curing (AC) is a concrete curing method widely used for the production of precast concrete components, especially prestressed, high-strength, concrete pipe piles [1–3]. AC can achieve high concrete strength within a short time and, thus, considerably enhances the production efficiency of precast components [4]. In general, the strength of concrete is proportional to its durability performance, that is, the higher the strength of concrete, the stronger its durability performance [5]. However, in some cases, the high strength of concrete achieved by AC does not warrant enhanced durability [3,6,7]. Consequently, scholars have used several methods to improve the durability properties of AC concrete, including incorporating mineral admixtures or adjusting curing parameters in the AC regime [8–11]. However, the above methods are either inefficient or too complex, a new, simple, and effective method requires further research. The emergence of nanomaterials brings hope for the improvement of durability properties of AC concrete.

Various nanomaterials have been applied to concrete to improve its properties [12–29]. Nano-SiO_2, for example, has been extensively studied due to its small-size effects and high pozzolanic activity. Suitable replacement with nano-SiO_2 can effectively enhance the mechanical properties and durability performance of concrete [14–18]. Nanomaterials generally have many beneficial effects, but they are often rare and expensive; by contrast, concrete is an inexpensive and broadly consumed construction material. Adding expensive nanomaterials to concrete inevitably increases its cost, which is disadvantageous for the application of nanomaterials to concrete engineering. Compared with nano-SiO_2, nano$CaCO_3$ (NC) has a much lower production cost, stable performance, and abundant supply; hence, the latter is more practical for concrete applications than the former [21–27].

Liu et al. [21] studied the effect of NC on the properties of cement paste and found that NC reduces the

flowability and setting time of fresh cement paste; the group found 1% NC to be the optimal amount to improve the mechanical properties of hardened cement. Shaikh and Supit [22] investigated the effects of NC on the mechanical and durability performance of concrete with a high volume of fly ash under room-temperature water curing; they also found that a 1% NC replacement ratio results in remarkable improvements in the compressive strength, porosity, water sorptivity, chloride permeability, and chloride ion diffusivity of concrete. Li et al. [23] studied the strength and microstructure of ultra-high-performance concrete with different NC replacement levels under standard curing (SC) conditions and discovered that replacement with 3% NC results in optimal compressive strength. NC acts as an inert filling that creates a dense microstructure in concrete and accelerates cement hydration through the boundary nucleation growth effect. Wu et al. [5,24] studied the effects of NC on the mechanical properties and microstructure of ultra-high-performance concrete cured in 20°C lime-saturated water and found that an optimal replacement of 3.2% NC exerts nucleation and filling effects; the NC reacts with tricalcium aluminate to form carboaluminates, resulting in low porosity and more homogeneous structures in concrete. Similar studies [25–27] have also reported that a suitable level of NC replacement in concrete helps prevent carbonation, frost, and sulfate erosion.

The aforementioned studies on NC in concrete were mostly conducted under normal-temperature curing conditions, and the application of NC to concrete under AC conditions has been seldom performed. Given the large difference of concrete between under normal-temperature curing and AC conditions [2,3,28], whether NC plays a beneficial role in AC concrete similar to its effects on ordinary cured concrete must be investigated. This study replaced part of the cement in concrete with 1, 2, and 3% NC to investigate the effects of such replacement on the carbonation and chloride resistance of hardened AC concrete. The obtained AC concrete exhibited excellent durability properties.

2 Materials and testing methods

2.1 Raw materials

In accordance with Chinese standard GB 175-2007 (Common Portland Cement), P·II 52.5 Portland cement, the chemical composition of which is given in Table 1, was used as the concrete binder. Local river sand with a fineness modulus of 2.4 and a specific gravity of 2.69 was utilized as the fine aggregate, and crushed limestone with a 5–25 mm continuous gradation size and 2.64 specific gravity was adopted as the coarse aggregate. Common tap water was used as the mixing water. A type of polycarboxylate superplasticizer was utilized as the chemical admixture, and the water/cement ratio of concrete was set to 0.27. The basic mixture proportions of cement, water, fine aggregate, coarse aggregate, and chemical admixture are 450, 120, 680, 1,320, and 9 kg/m^3, respectively.

Table 1: Chemical composition of cement (%)

Item	SiO_2	SO_3	Fe_2O_3	Al_2O_3	CaO	MgO	Loss of ignition
Content	22.3	3.7	3.3	5.1	64.7	0.9	1.2

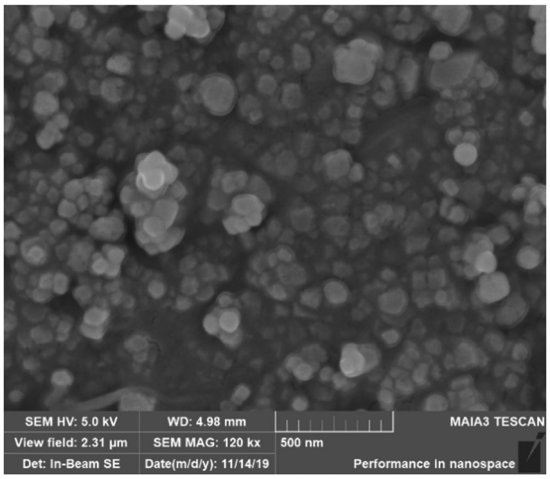

Figure 1: SEM image of NC powder.

Ordinary NC powder was purchased from the market and used to replace cement at three levels of 1, 2, and 3%. According to the information provided by the manufacturer, such NC material is a white powder with a net content of 99% and pH value of 8–10, and its particle size range is 10–50 nm and specific surface area is 80–200 m^2/g. The scanning electronic microscopy (SEM) image of NC powder is shown in Figure 1, which is consistent with its particle size.

2.2 Specimen fabrication and curing methods

Sufficient dispersion of a nanomaterial is key to fully maximize its functions in concrete [29,30]. In this study, NC-modified concrete was mixed as follows [31]. First, NC powder was added to mixing water and stirred

continuously with a glass rod until an even colloidal suspension was formed. Next, 0.2% tributyl phosphate, 0.1% sodium citrate (by weight of cement), and the chemical admixture were added to the nanosolution and mixed with a mechanical stirrer for 5 min. Third, cement was added to the mixing solution and mixed evenly until a uniform cement slurry was formed. Fourth, the fine aggregate was added to the prepared cement slurry and mixed for 2 min in a forced drum mixer to form cement mortar. Finally, the coarse aggregate was placed in the cement mortar and mixed fully for 5 min to create NC-modified concrete.

Two types of specimens were prepared: (1) a 100 × 100 × 100 mm^3 cubic specimen for concrete accelerated carbonation experiments and (2) a ϕ100 × 50 mm^3 cylinder specimen for concrete Coulomb electrical flux experiments. Fresh concrete was poured into plastic molds and compacted using a vibrating table. The specimens were then placed in an indoor environment and maintained with sufficient moisture for 24 h before demolding. Two curing methods of AC and SC (for comparison) were utilized: (1) AC comprising initial steam curing for 6.5 h (90 ± 5°C), followed by AC for 6 h (180 ± 5°C, 1.0 ± 0.05 MPa) [11] and (2) SC (T = 20 ± 2°C, RH ≥ 95%) for 28 d. After curing, the specimens were obtained and placed in an indoor natural environment (T = 14.5 ± 4.5°C, RH = 71 ± 10%) until different designed ages for further experiments.

2.3 Experimental methods

To obtain the long-term durability behaviors of NC modified autoclaved concrete, specimens' accelerated carbonation and Coulomb electric flux experiments were conducted at their ages of 28, 90, 180, and 300 d according to GB/T 50082-2009 (Standard for Test Methods of Long-term Performance and Durability of Ordinary Concrete). The temperature, relative humidity, and CO_2 concentration in the chamber used for the carbonation test were set to 20 ± 2°C, 70 ± 5%, and 20 ± 3%, respectively. To save the experimental time, the carbonation time was set to 10 d. The carbonation depth of concrete was tested using 1% phenolphthalein ethanol indicator and measured with a Vernier caliper. To reduce errors usually occurred in autoclaved concrete specimens caused by solution overheating during the Coulomb electric flux experiment [6,11], the Coulomb charges of concrete were determined using an improved method of multiplying the initial charges of 30 min by 12 [28,32]. In addition, the compressive strength of concrete specimens at the ages of 28 and 300 d was also conducted according to the standard of GB/T 50081-2002 (Standard for Test Method of Mechanical Properties on Ordinary Concrete). In all experiments, three specimens were taken as a group, and the mean value of the three specimens was taken as a representative value of the group.

X-ray diffraction (XRD; D8 ADVANCE X-ray diffractometer, BRUKER Company, Germany), thermogravimetry (TG; Discovery TGA thermogravimetric analyzer, TA Company, USA), SEM (Quanta 250 scanning electron microscope, FEI Company, USA), and mercury intrusion porosimetry (MIP; AUTOPORE IV 9510 mercury injection apparatus, Mike Company, USA) were also performed to study the effects of NC on the hydration products of AC or SC cement and microscopic pore structures in AC or SC concrete. The samples used for the XRD, TG, and SEM tests were hardened cement pastes with the same water/cement ratio and cured under the same conditions as the corresponding concrete specimens, and the samples for the MIP test were 5–8 mm mortar pieces extracted from concrete. All samples were stored in anhydrous ethanol to terminate further hydration at the ages of 28 and 300 d and dried in an oven at 60°C for 24 h prior to examination. In addition, samples used for XRD and TG were ground and passed through a 200-mesh sieve.

3 Results and discussion

3.1 Carbonation resistance of AC concrete with NC

Generally speaking, the durability of concrete is closely related to its strength. Table 2 presents the 28 and 300 d compressive strength of concrete with different NC replacement ratios. Table 2 shows that the 28 d strength of AC concrete is usually higher than that of SC concrete, while the 300 d strength of AC concrete is usually lower than that of SC concrete. It fully reflects the strength development characteristics of AC concrete [11]. In addition, the strength of NC-modified concrete is usually just a little higher than that of the control concrete (0% NC), and 1% NC-modified concrete obtains the highest strength [21,22].

The initial carbonation depths of specimens before accelerated carbonation experiment were measured, and they were all very small even for specimens at the age of 300 d, thus they could be ignored. The accelerated carbonation depths of SC and AC concrete replaced with

Table 2: Compressive strength of concrete with different NC replacement ratios (MPa)

Item	Age/d	NC replacement ratio			
		0%	1%	2%	3%
AC	28	72.9	75.5	72.8	70.9
	300	69.2	75.1	73.1	69.3
SC	28	59.8	66.3	60.7	63.3
	300	78.4	82.2	78.2	74.3

different amounts of NC are presented in Figure 2. The two curing conditions exerted considerable effects on the carbonation resistance of the resulting concrete. AC is expected to substantially increase the porosity of concrete due to its high curing temperature and pressure [3,11]; therefore, although AC concrete usually has higher strength relative to SC concrete, AC concrete exhibits poorer durability performance than that of SC concrete, including carbonation resistance of concrete. In this study, the respective carbonation depths of AC concrete (0% NC) at the ages of 28 and 300 d were 3.1 and 7.9 times, respectively, than that of SC concrete (0% NC). This result confirms that AC greatly reduces the carbonation resistance of concrete [3,11,28].

Although NC is not a pozzolanic material, its fine particles can help increase the packing density of concrete and, thus, contributes to the carbonation resistance of the material [33,34]. The following observations can be made from Figure 2. Regardless of the curing condition, the carbonation depth of concrete with NC was consistently lower than that of the corresponding control concrete (0% NC). The AC concrete samples had higher carbonation depths than their counterpart SC concrete samples. Without NC, the carbonation depths of SC concrete decreased with concrete age, whereas those of AC concrete slightly increased.

The carbonation depths of NC-modified SC and AC concrete usually decreased with concrete age and increasing NC replacement, except at 28 and 90 d ages. It may be due to that the beneficial effects of NC take time to develop [5,24]. Before the age of 90 d, the negative effects of AC prevailed. Thus, the carbonation depths of NC-modified AC concrete at 90 d are even higher than that at 28 d (Figure 2b). However, with the increasing of concrete age, the beneficial effect of NC took over. As a result, the carbonation depth of NV-modified AC concrete is getting lower and lower.

At the age of 300 d, the improvement in the carbonation resistance of AC concrete with 1, 2, and 3% NC reached 54.5, 59.5, and 66.8%, respectively, and these results suggest that 3% NC replacement most effectively enhances the long-term carbonation resistance of concrete. Although the carbonation depths of NC-modified AC concrete remained higher than those of SC concrete, they were closer to those of SC concrete than to that of unmodified AC concrete. Thus, the application of NC could confer substantial improvements in the carbonation resistance of AC concrete.

3.2 Chloride resistance of AC concrete with NC

The Coulomb electric fluxes of concrete samples of different ages and with different NC replacement levels are shown in Figure 3. NC generally enhanced the chloride resistances of the SC and AC concretes, although the Coulomb charges of AC concrete were higher than those of SC concrete. Specifically, the respective Coulomb charges of the control AC concrete (0% NC) at the ages of 28 and 300 d were 1.5 and 3 times the corresponding charges of SC concrete. Interestingly, the trends of NC effects on the Coulomb electric fluxes of the concrete were similar to those on carbonation depths, that is, 3% NC replacement is the optimal dosage for improving the long-term chloride resistance of concrete. At the age of 300 d, the improvement in the

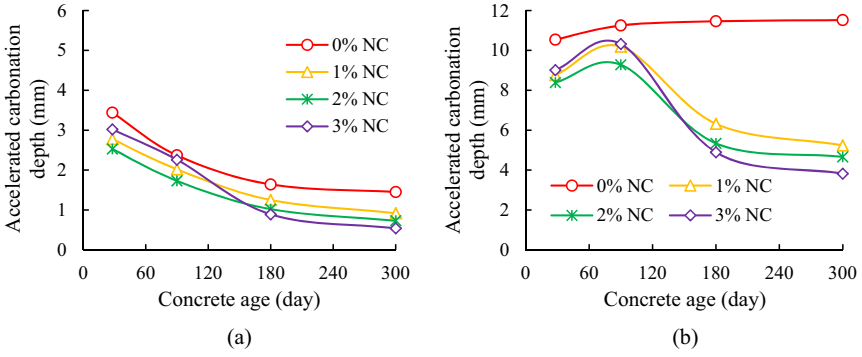

Figure 2: Concrete accelerated carbonation depths with different levels of NC replacement (a) SC concrete (b) AC concrete.

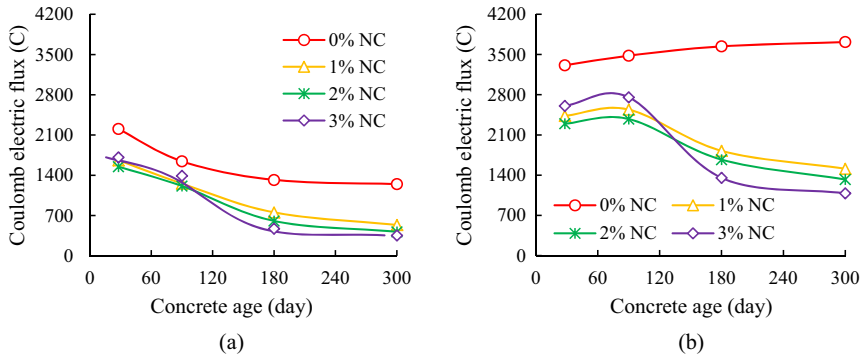

Figure 3: Concrete Coulomb electric fluxes with different levels of NC replacement. (a) SC concrete (b) AC concrete.

chloride resistance of AC concrete with 1, 2, and 3% NC reached 59.3, 64.4, and 70.8%, respectively. The Coulomb values of 3% NC-modified AC concrete became even lower than those of SC concrete (0% NC), thus suggesting that the application of NC exerts substantial improvements in the chloride resistance of AC concrete.

As shown in Figures 2 and 3, before the age of 90 d, 2% is the optimal NC replacement ratio for enhancing the anticarbonation and antichloride performance of SC and AC concrete. However, with the continued increase of concrete age, 3% become the optimal NC replacement level for AC and SC concrete to achieve maximum chloride and carbonation resistance. Such phenomenon has not been found in the previous references. The possible reason lies in that NC plays both filling effect and nucleation effect in concrete [21–27], which will be discussed in detail in the following sections. At the ages of 28 and 90 d, 2% NC behaved the best, while too much replacement (3% NC) easily caused agglomeration, and decreased concrete durability performance. With the increasing of concrete age, the nucleation effect of NC began to increase, which promoted the hydration of residual unhydrated cement particles in concrete, and the newly formed cement hydrated products diluted the agglomeration of NC particles. Finally, the anticarbonation and antichloride performance of 3% NC-modified AC concrete exceeded that of 2% NC-modified AC concrete.

There is a peculiar phenomenon of different optimal dosages of NC for concrete strength and durability performance, which may be ascribed to that the control mechanisms to concrete strength and durability performance are different. The control factor to concrete strength is mainly the quality of the interfacial transition zone (ITZ) between coarse aggregate and mortar in concrete [35,36], while that to concrete carbonation and chloride resistance mainly depends on the microscopic pore structures in concrete [3,7,11]. When 1% NC was utilized, it can effectively improve the quality of ITZ, thus the highest concrete strength was obtained [21,22]. When 3% NC was utilized, it can effectively improve concrete micropore structures, thus the best durability performance was obtained [23,24].

3.3 Hydration products of AC cement with NC

For convenience of expression, the control samples (cement paste or mortar with 0% NC) obtained under SC and AC conditions are hereinafter referred to as SC0 and AC0, respectively, and the corresponding AC sample with 3% NC is referred to as ACNC. The XRD patterns of SC0, AC0, and ACNC at the ages of 28 and 300 d are shown in Figure 4. The compositions of the hydration products of the three samples were similar, although tobermorite only appeared in AC0 and ACNC.

The intensity of the diffraction peak of $Ca(OH)_2$ in ACNC is much higher than that in AC0; by comparison, the corresponding peak in AC0 is higher than that in SC0. The hydration degree of AC0 is higher than that of SC0, and NC promotes the hydration degree of AC cement further. Theoretically, there should be no calcite crystal in hardened cement paste of SC0. However, $Ca(OH)_2$ was easily carbonated in a natural air environment due to the ground particles of hardened cement paste. TG tests were conducted to quantitatively analyze the composition of the hydration products of the three cement paste samples, and the corresponding TG and differential thermogravimetry (DTG) curves are presented in Figure 5.

Free water in the cement paste evaporates from room temperature to 100°C. The C–S–H gel, AFt, and $Ca(OH)_2$ crystals decompose and release bound water (*i.e.* chemical combined water) at 80–90, 130, and 380–500°C, respectively, and calcite crystals decompose and release

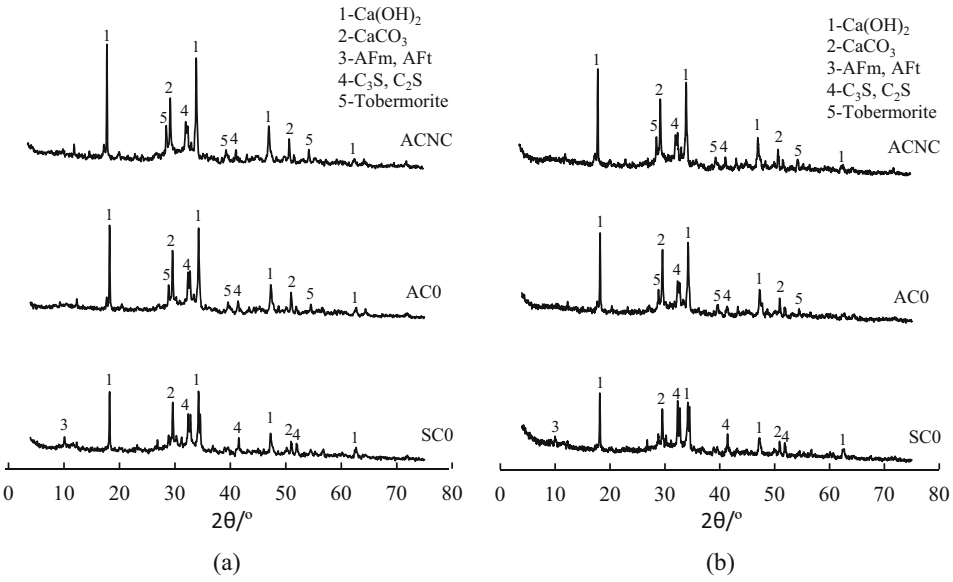

Figure 4: XRD patterns of cement paste samples at different ages (a) 28 d (b) 300 d.

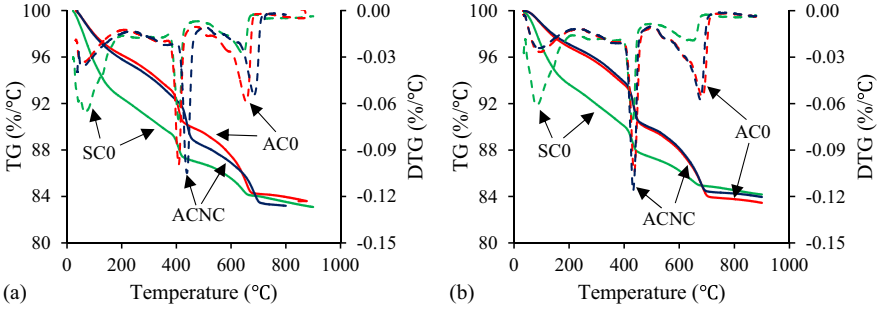

Figure 5: TG–DTG curves of different cement paste samples at different ages (a) 28 d (b) 300 d.

CO_2 gas at 600–700°C [2,10,37]. In addition, tobermorite loses its four interlayer water molecules at 50–300°C, Si–O–H bonds are cleaved, and dihydroxylation occurs at 724°C [38]. Therefore, the decomposition peak of calcite overlaps that of tobermorite. Because there is no tobermorite in SC0 sample, the content of calcite in SC0 can be determined first. It was assumed that the same carbonation degree occurred in the samples of SC0, AC0, and ACNC. Then, the contents of tobermorite in AC0 and ACNC could be distinguished. The contents of the main hydration products of the samples were calculated based on the above mechanisms and the TG-DTG data, and the results are listed in Table 3.

As indicated in Table 3, the hydration products of cement differed under varying curing conditions. The hydration products of SC cement were mainly $Ca(OH)_2$ and C–S–H gel without tobermorite, while those in AC cement were mainly $Ca(OH)_2$, tobermorite, and a small amount of

Table 3: Main hydration products of different cement samples based on TG tests

Sample	Age (d)	Bound water (%)	$Ca(OH)_2$ (%)	Tobermorite (%)	C–S–H (%)
SC0	28	8.76	10.85	0.00	38.18
AC0	28	8.50	15.21	32.53	8.16
ACNC	28	9.53	18.00	36.16	7.76
SC0	300	9.60	12.70	0.00	41.08
AC0	300	9.11	17.83	30.58	9.56
ACNC	300	9.02	18.19	33.61	12.67

C–S–H gel. Several changes in the composition of the hydration products of AC cement occurred after replacement with 3% NC. Specifically, the content of tobermorite in ACNC at 28 d increased by 11.2%, and the content of C–S–H gel in ACNC at 300 d increased by 32.5%, relative to those in AC0. This finding confirms that, although NC does not have pozzolanic activity, it exerts an accelerating effect and promotes cement hydration both in the AC period and the later period, thus producing more hydration products in cement [24,39,40].

As the concrete age increased from 28 to 300 d, the hydration products of the cement samples remained the same, but their contents changed slightly. The contents of $Ca(OH)_2$ and C–S–H gel increased in all samples; this result may be ascribed to the ongoing hydration of residual unhydrated cementitious particles in the concrete, which generates more of these products. By contrast, the contents of tobermorite in AC0 and ACNC slightly decreased, which may be due to the transformation of metastable phases in the silicate hydrate [41].

3.4 Effects of NC on the micromorphology of AC cement

SEM images of SC0, AC0, and ACNC samples at the ages of 28 and 300 d are presented in Figure 6.

SC can usually provide the appropriate temperature and sufficient moisture for cement hydration so that hydration can proceed completely and the most compact microstructure in concrete can be obtained [42,43]. By comparison, the high-temperature and -pressure conditions in AC dramatically promote the hydration speed of cement; however, it also restrains the uniform distribution of hydration products due to the short period for hardening [3,7,44]. SC0 is very dense (Figure 6a), whereas AC0 is relatively porous (Figure 6b). Interestingly, the AC cement microstructure became compact after replacement with 3% NC (Figure 6c). This result suggests that NC exerts crystal nucleus and filling effects to improve the compactness of concrete. In addition, NC may react with tricalcium aluminate to form calcium carboaluminate hydrate [24,45],

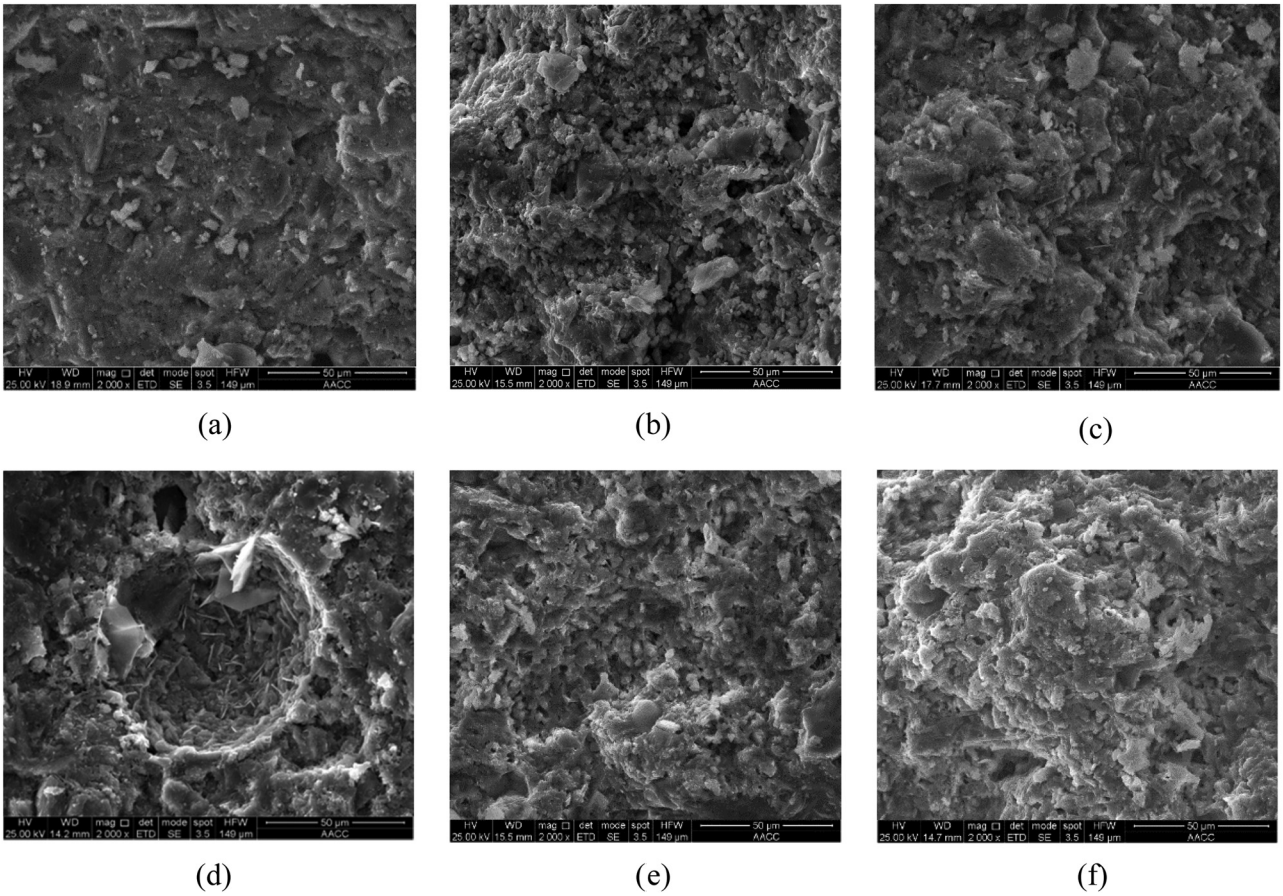

Figure 6: SEM images of cement paste samples at different ages (a) SC0 (28 d) (b) AC0 (28 d) (c) ACNC (28 d) (d) SC0 (300 d) (e) AC0 (300 d) (f) ACNC (300 d).

which is also beneficial to enhance the compactness of concrete.

As the concrete age increases, residual unhydrated cement particles in concrete continue to hydrate, and the microstructure of cement becomes increasingly compact. However, the moisture content of AC concrete was low due to large amount of water lost during cooling [11]. Thus, subsequent hydration of cement in AC concrete was not evident, and the compactness of AC0 remained nearly the same at the ages of 28 and 300 d (Figures 6b and e).

Table 4: MIP results of the concrete samples

Sample		Porosity (%)	Average pore diameter (nm)	Most probable aperture (nm)	Medium pore diameter (nm)
SC0	28 d	8.79	24.8	26.3	67.2
	300 d	8.53	26. 9	26.3	53.3
AC0	28 d	10.88	37.1	3.2	382.7
	300 d	10.81	30.5	52.5	200.1
ACNC	28 d	9.51	23.2	32.4	170.4
	300 d	9.32	20.1	29	153.1

3.5 Effects of NC on the pore structures of AC concrete

Given that microscopic pores in concrete serve as channels through which an external corrosive medium can enter the material, the micropore characteristics of concrete play a decisive role in its durability performance [24,27,46,47]. Figure 7 presents the pore-size distribution results of SC0, AC0, and ACNC samples at the ages of 28 and 300 d. Different curing methods and the incorporation of NC produced remarkable influences on the micropore structure of concrete. Based on MIP results, concrete porosity and other pore-size information of the three concrete samples are listed in Table 4.

From Table 4, the micropore structural data of all samples at the ages of 28 and 300 d are similar, although the values at 300 d are generally lower than those at 28 d. Specifically, the porosity and average pore diameter of AC0 at 28 d increased by 23.8 and 49.6%, respectively, when compared with those of SC0. After incorporation of 3% NC, the porosity and average pore diameter of ACNC decreased by 12.6 and 37.3% at 28 d, and 13.8 and 34.1% at 300 d, respectively. Additionally, the most probable aperture and the medium pore diameter of ACNC at 300 d also decreased by 44.8 and 23.5%. The aforementioned substantial improvements of micropore structure in ACNC imply that the AC concrete is getting denser and its impermeability becomes higher, which agrees well with the carbonation depth and Coulomb value data of AC concrete shown in Figures 2b and 3b.

Considering that porosity and average pore diameter cannot fully reflect the characteristics of a porous medium, Wu and Lian [48] proposed the following types of micropores: high-harm pores (>200 nm), moderate-harm pores (50–200 nm), low-harm pores (20–50 nm), and harmless pores (<20 nm). The pore diameter ratios of SC0, AC0, and ACNC obtained from the MIP results are plotted and shown in Figure 8. Moderate- and high-harm pores, which have deleterious or severely deleterious effects on concrete performance, can be classified as large pores, whereas low-harm and harmless pores, which have no adverse or only slight adverse effects, can be classified as small pores [49–51].

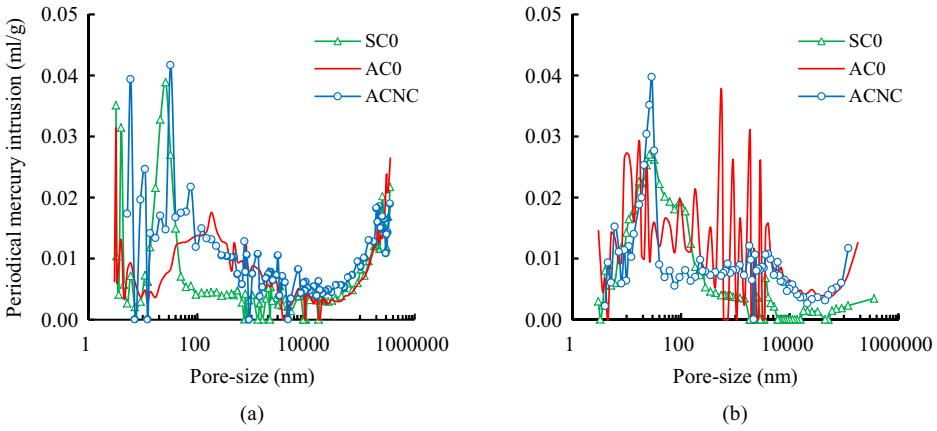

Figure 7: Pore-size distribution of different concrete samples (a) 28 d (b) 300 d.

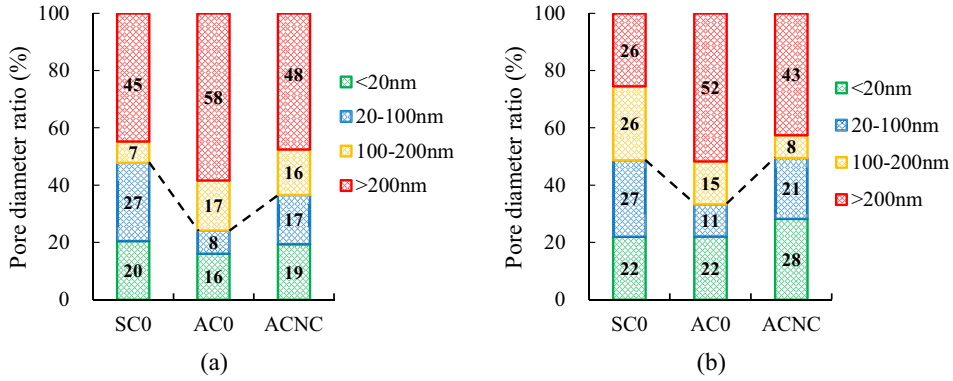

Figure 8: Pore diameter distributions in samples at different ages (a) 28 d (b) 300 d.

As shown in Figure 8a, AC significantly increased the proportion of large pores in the concrete samples from 52% (SC0) to 75% (AC0). After replacement with 3% NC, the proportion of large pores was reduced to 64% (ACNC). This finding explains why AC deteriorates the durability performance of concrete significantly whereas NC improves the durability performance of AC concrete effectively. Even at 300 d (Figure 8b), the proportion of large pores in AC0 remained the highest (67%) among the three samples, whereas that in ACNC remained the lowest (51%). NC effectively refined the micropores in AC concrete, resulting in short- and long-term anticarbonation and antichloride performance improvements.

4 Conclusions

Based on the experimental results and analyses, it confirms that the application of NC can substantially enhance the carbonation and chloride resistances of AC concrete such that they approach or even exceed those of SC concrete, thus it provides a new method to improve the anticarbonation and antichloride performance of AC concrete.

Different NC replacement levels usually produce different improvements. Among the three NC replacement ratios, the 3% NC replacement is the optimal dosage for improving the long-term carbonation or chloride resistance of concrete. At the age of 300 d, the improvements in the carbonation and chloride resistance of AC concrete with 3% NC are 66.8 and 70.8%, respectively.

The key mechanism of NC in improving the durability performance of AC concrete involves reduction of concrete porosity and proportion of large pores, refinement of the micropores in AC concrete through the effects of filling, and acceleration of cement hydration production.

Acknowledgements: The authors are grateful for the financial support from the National Natural Science Foundation of China (grant number 51979169); device support from the Advanced Analysis & Computation Center of China University of Mining & Technology.

Conflict of interest: The authors declare no conflict of interest regarding the publication of this paper.

References

[1] Yazıcı H, Yiğiter H, Aydın S, Baradan B. Autoclaved SIFCON with high volume class C fly ash binder phase. Cem Concr Res. 2006;36(3):481–6.

[2] Alhozaimy A, Fares G, Al-Negheimish A, Jaafar MS. The autoclaved concrete industry: An easy-to-follow method for optimization and testing. Constr Build Mater. 2013;49:184–93.

[3] Liu Z, Bu L, Wang Z, Hu G. Durability and microstructure of steam cured and autoclaved PHC pipe piles. Constr Build Mater. 2019;209:679–89.

[4] Joo M, Ohama Y, Yeon KS. Strength properties of autoclaved and combined wet/dry-cured SBR-modified concretes using ground granulated blast-furnace slag. Mag Concr Res. 2004;56(9):513–21.

[5] Wu Z, Shi C, Khayat KH, Wan S. Effects of different nanomaterials on hardening and performance of ultra-high strength concrete (UHSC). Cem Concr Compos. 2016;70:24–34.

[6] Aldea C-M, Young F, Wang K, Shah SP. Effects of curing conditions on properties of concrete using slag replacement. Cem Concr Res. 2000;30(3):465–72.

[7] Tan K, Zhu J. Influences of steam and autoclave curing on the strength and chloride permeability of high strength concrete. Mater Struc. 2017;50:56.

[8] Wongkeo W, Thongsanitgarn P, Pimraksa K, Chaipanich A. Compressive strength, flexural strength and thermal conductivity of autoclaved concrete block made using bottom ash as cement replacement materials. Mater Des. 2012;35:434–9.

[9] Yazıcı H, Deniz E, Baradan B. The effect of autoclave pressure, temperature and duration time on mechanical properties of reactive powder concrete. Constr Build Mater. 2013;42:53–63.
[10] Alawad OA, Alhozaimy A, Jaafar MS, Abdul Aziz FN, Al-Negheimish A. Effect of autoclave curing on the microstructure of blended cement mixture incorporating ground dune sand and ground granulated blast furnace slag. Int J Concr Struct M. 2015;9(3):381–90.
[11] Li G, Gao X. Effects of secondary water curing on the long-term strength and durability of concrete after steam-autoclave curing. J Southeast Uni (Eng Ed). 2018;34(4):488–94.
[12] Camiletti J, Soliman AM, Nehdi ML. Effect of nano-calcium carbonate on early-age properties of ultra-high-performance concrete. Mag Concr Res. 2013;65(5):297–307.
[13] Fan Y, Zhang S, Wang Q, Shah SP. Effects of nano-kaolinite clay on the freeze–thaw resistance of concrete. Cem Concr Compos. 2015;62:1–12.
[14] Zhang H, Zhao Y, Meng T, Shah SP. The modification effects of a nano-silica slurry on microstructure, strength, and strain development of recycled aggregate concrete applied in an enlarged structural test. Constr Build Mater. 2015;95:721–35.
[15] Ghafari E, Arezoumandi M, Costa H, Júlio E. Influence of nano-silica addition on durability of UHPC. Constr Build Mater. 2015;94:181–8.
[16] Amin M, Bassuoni MT. Response of concrete with blended binders and nanoparticles to sulfuric acid attack. Mag Concr Res. 2018;70(12):617–32.
[17] Zhang P, Li Q, Wang J, Shi Y, Ling Y. Effect of PVA fiber on durability of cementitious composite containing nano-SiO_2. Nanotechnol Rev. 2019;8:116–27.
[18] He K, Chen Y, Xie W. Test on axial compression performance of nano-silica concrete-filled angle steel reinforced GFRP tubular column. Nanotechnol Rev. 2019;8:523–38.
[19] Bukit N, Ginting EM, Hutagalung EA, Sidebang E, Frida E, Bukit BF. Preparation and characterization of oil palm ash from boiler to nanoparticle. Rev Adv Mater Sci. 2019;58: 195–200.
[20] Zhuang C, Chen Y. The effect of nano-SiO_2 on concrete properties: a Review. Nanotechnol Rev. 2019;8:562–72.
[21] Liu X, Chen L, Liu A, Wang X. Effect of nano-$CaCO_3$ on properties of cement paste. Energy Procedia. 2012;16:991–6.
[22] Shaikh FUA, Supit SWM. Mechanical and durability properties of high volume fly ash (HVFA) concrete containing calcium carbonate ($CaCO_3$) nanoparticles. Constr Build Mater. 2014;70:309–21.
[23] Li W, Huang Z, Cao F, Sun Z, Shah SP. Effects of nano-silica and nano-limestone on flowability and mechanical properties of ultra-high-performance concrete matrix. Constr Build Mater. 2015;95:366–74.
[24] Wu Z, Shi C, Khayat KH. Multi-scale investigation of microstructure, fiber pullout behavior, and mechanical properties of ultra-high performance concrete with nano-$CaCO_3$ particles. Cem Concr Compos. 2018;86:255–65.
[25] Sato T, Beaudoin JJ. Effect of nano-$CaCO_3$ on hydration of cement containing supplementary cementitious materials. Adv Cem Res. 2011;23(1):33–43.
[26] Wang D, Meng Y, Li T. Experiments about the application of nano-SiO_2 and nano-$CaCO_3$ to improve the frost resistance of concrete. China Concr Cem Products. 2015;7:6–10.
[27] Meng T, Yu Y, Wang Z. Effect of nano-$CaCO_3$ slurry on the mechanical properties and micro-structure of concrete with and without fly ash. Compos Part B-Eng. 2017;117:124–9.
[28] Li G, Zhou J, Yue J, Gao X, Wang K. Effects of nano-SiO_2 and secondary water curing on the carbonation and chloride resistance of autoclaved concrete. Constr Build Mater. 2020;235:117465.
[29] Hu T, Jing H, Li L, Yin Q, Shi X, Zhao Z. Humic acid assisted stabilization of dispersed single-walled carbon nanotubes in cementitious composites. Nanotechnol Rev. 2019;8:513–22.
[30] Hashim H, Salleh MS, Omar MZ. Homogenous dispersion and interfacial bonding of carbon nanotube reinforced with aluminum matrix composite: a review. Rev Adv Mater Sci. 2019;58:295–303.
[31] Wei H. Study on effect and mechanism of nano-$CaCO_3$ in cement-based materials [Dissertation]. Harbin Institute of Technology; 2013.
[32] McGrath PF, Hooton RD. Re-evaluation of the AASHTO T259 90-day salt ponding test. Cem Concr Res. 1999;29(8):1239–48.
[33] Ying S, Qian X, Zhan S. Effect of nano-$CaCO_3$ on the properties of autoclaved aerated concrete. Bull Chin Ceram Soc. 2011;30(6):1254–9.
[34] Ming X, Ming X. Influence of conventional dispersed nano-$CaCO_3$ on performance of concrete. J Highw Transport Res Dev. 2019;36(6):25–30.
[35] Poon CS, Shui ZH, Lam L. Effect of microstructure of ITZ on compressive strength of concrete prepared with recycled aggregates. Constr Build Mater. 2004;18(6):461–8.
[36] Königsberger M, Hlobil M, Delsaute B, Staquet S, Hellmich C, Pichler B. Hydrate failure in ITZ governs concrete strength: A micro-to-macro validated engineering mechanics model. Cem Concr Res. 2018;103:77–94.
[37] Reiterman P, Holčapek O, Zobal O, Keppert M. Freeze-thaw resistance of cement screed with various supplementary cementitious materials. Rev Adv Mater Sci. 2019;58:66–74.
[38] Yang X, Cui X, Cui C, Ma H, Yang Q. Study on high-temperature phase change of tobermorite. Spectrosc Spectr Anal. 2013;33(8):2227–30.
[39] Péra J, Husson S, Guilhot B. Influence of finely ground limestone on cement hydration. Cem Concr Compos. 1999;21(2):99–105.
[40] Bonavetti VL, Rahhal VF, Irassar EF. Studies on the carboaluminate formation in limestone filler-blended cements. Cem Concr Res. 2001;31(6):853–9.
[41] Luke K. Phase studies of pozzolanic stabilized calcium silicate hydrates at 180°C. Cem Concr Res. 2004;34(9):1725–32.
[42] Reinhardt H-W, Stegmaier M. Influence of heat curing on the pore structure and compressive strength of self-compacting concrete (SCC). Cem Concr Res. 2006;36(5):879–85.
[43] Li G, Yao F, Liu P, Yan C. Long-term carbonation resistance of concrete under initial high-temperature curing. Mater Struct. 2016;49(7):2799–806.
[44] Kjellsen KO, Detwiler RJ, Gjørv OE. Development of microstructures in plain cement pastes hydrated at different temperatures. Cem Concr Res. 1991;21(1):179–89.
[45] De Weerdt K, Ben Haha M, Le Saout G, Kjellsen KO, Justnes H, Lothenbach B. Hydration mechanisms of ternary Portland cements containing limestone powder and fly ash. Cem Concr Res. 2011;41:279–91.

[46] Zhang P, Wittmann FH, Vogel M, Müller HS, Zhao T. Influence of freeze-thaw cycles on capillary absorption and chloride penetration into concrete. Cem Concr Res. 2017;100: 60–7.
[47] Guo K, Miao H, Liu L, Zhou J, Liu M. Effect of graphene oxide on chloride penetration resistance of recycled concrete. Nanotechnol Rev. 2019;8:681–9.
[48] Wu Z, Lian H. High performance concrete. Beijing: China Railway Publishing House; 1999.
[49] Zhang M-H, Li H. Pore structure and chloride permeability of concrete containing nano-particles for pavement. Constr Build Mater. 2011;25(2):608–16.
[50] Zhang B, Tan H, Shen W, Xu G, Ma B, Ji X. Nano-silica and silica fume modified cement mortar used as surface protection material to enhance the impermeability. Cem Concr Compos. 2018;92:7–17.
[51] Yu W, Tang H. Experimental study on the existence of nano-scale pores and the evolution of organic matter in organic-rich shale. Nanotechnol Rev. 2019;8:156–67.